

New Palladium(II) Complex of P,S-Containing Hybrid Calixphyrin. Theoretical Study of Electronic Structure and Reactivity for Oxidative Addition

Noriaki Ochi,[†] Yoshihide Nakao,[†] Hirofumi Sato,[†] Yoshihiro Matano,[†]
Hiroshi Imahori,^{†,‡,§} and Shigeyoshi Sakaki^{*,†,‡}

Department of Molecular Engineering, Graduate School of Engineering, Kyoto University,
Nishikyo-ku, Kyoto 615-8510, Japan, Fukui Institute for Fundamental Chemistry,
Nishihiraki-cho, Takano, Sakyo-ku 610-8103, Japan, and Institute for Integrated Cell-Material
Sciences (iCeMS), Kyoto University, Nishikyo-ku, Kyoto 615-8510, Japan

Received February 14, 2009; E-mail: sakaki@moleng.kyoto-u.ac.jp

Abstract: The palladium complex of P,S-containing hybrid calixphyrin **1** was investigated with the DFT method. There are two kinds of valence tautomer in **1**: one is a Pd(II) form in which the calixphyrin moiety possesses -2 charges and the Pd center takes $+2$ oxidation state, and the other is a Pd(0) form in which the calixphyrin is neutral and the Pd center takes zero oxidation state. Complex **1** takes the Pd(II) form in the ground state. Though the Pd center takes $+2$ oxidation state, DFT computations clearly show that the oxidative addition of phenyl bromide (PhBr) to **1** occurs with moderate activation enthalpy, as experimentally proposed. The first step of the oxidative addition is the coordination of PhBr with the Pd center to form intermediate **1INTa**, in which the Pd center and the calixphyrin moiety are neutral; in other words, the valence tautomerization from the Pd(II) form to the Pd(0) form occurs in the palladium calixphyrin moiety. The activation enthalpy is 22.5 kcal/mol, and the enthalpy change of reaction is 20.3 kcal/mol. The next step is the C–Br σ -bond cleavage of PhBr, which occurs with activation enthalpy of 2.0 kcal/mol relative to **1INTa**. On the other hand, the oxidative additions of PhBr to palladium complex of P,S-containing hybrid porphyrin **2** and that of conventional porphyrin **3** need much larger activation enthalpies of 49.1 and 74.4 kcal/mol, respectively. The differences in the reactivity among **1**, **2**, and **3** were theoretically investigated; in **1**, the valence tautomerization occurs with moderate activation enthalpy to afford the Pd(0) form which is reactive for the oxidative addition. In **2**, the tautomerization from the Pd(II) form to the Pd(0) form needs very large activation enthalpy (43.3 kcal/mol). In **3**, such valence tautomerization does not occur at all, indicating that the Pd(II) must change to the Pd(IV) in the oxidative addition of PhBr to **3**, which is a very difficult process. These differences are interpreted in terms of the π^* orbital energies of P,S-containing hybrid calixphyrin, hybrid porphyrin, and conventional porphyrin and the flexibility of their frameworks.

Introduction

Calixphyrin¹ is porphyrin analogue which contains several pyrroles bridged by sp^2 - and sp^3 -hybridized meso carbon atoms, as shown in Scheme 1A. This macrocyclic compound attracts considerable attention in porphyrin chemistry, host–guest chemistry, and coordination chemistry,^{2–5} because its π -conjugation is partially interrupted by the sp^3 -hybridized meso carbon, which leads to conformational flexibility of the mac-

rocyclic frame.⁶ Core-modified porphyrin is also promising, in which the nitrogen atoms of pyrrole moieties are substituted for heteroatoms such as phosphorus and sulfur atoms.⁷ Considering these two promising porphyrin analogues, heteroatom-

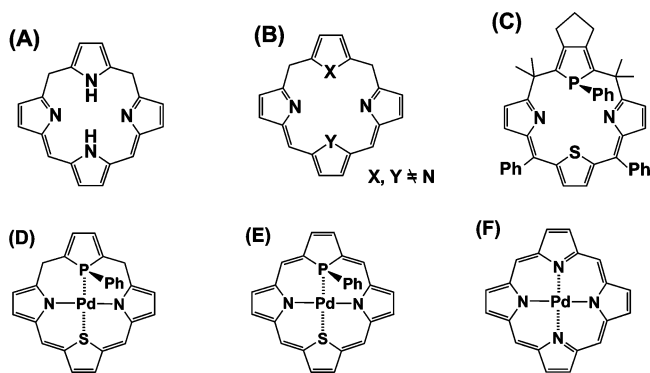
- (4) (a) Benech, J.-M.; Bonomo, L.; Solari, E.; Scopelliti, R.; Floriani, C. *Angew. Chem., Int. Ed.* **1999**, *38*, 1957. (b) Bonomo, L.; Toranman, G.; Solari, E.; Scopelliti, R.; Floriani, C. *Organometallics* **1999**, *18*, 5198.
- (5) (a) Krattinger, B.; Callot, H. J. *Tetrahedron Lett.* **1998**, *39*, 1165. (b) Harmjan, M.; Gill, H. S.; Scott, M. J. *J. Org. Chem.* **2001**, *66*, 5374. (c) Bucher, C.; Devillers, C. H.; Moutet, J.-C.; Pécaut, J.; Royal, G.; Saint-Aman, E.; Thomas, F. *Dalton Trans.* **2005**, 3620. (d) O'Brien, A. Y.; McGann, J. P.; Geier, G. R., III. *J. Org. Chem.* **2007**, *72*, 4084.
- (6) (a) Bucher, C.; Seidel, D.; Lynch, V.; Král, V.; Sessler, J. L. *Org. Lett.* **2000**, *2*, 3103. (b) Dolenský, B.; Kroulík, J.; Král, V.; Sessler, J. L.; Dvořáková, H.; Bouř, P.; Bernátková, M.; Bucher, C.; Lynch, V. *J. Am. Chem. Soc.* **2004**, *126*, 13714. (c) Bernátková, M.; Dvořáková, H.; Andrioletti, B.; Král, V.; Bouř, P. *J. Phys. Chem. A* **2005**, *109*, 5518.
- (7) Review: (a) Chandrashekar, T. K.; Venkatraman, S. *Acc. Chem. Res.* **2003**, *36*, 676. (b) Sessler, J. L.; Seidel, D. *Angew. Chem., Int. Ed.* **2003**, *42*, 5134. (c) Srinivasan, A.; Furuta, H. *Acc. Chem. Res.* **2005**, *38*, 10. (d) Chmielewski, P. J.; Latos-Grafiński, L. *Coord. Chem. Rev.* **2005**, *249*, 2510. (e) Gupta, I.; Ravikanth, M. *Coord. Chem. Rev.* **2006**, *250*, 468, and references therein.

[†] Department of Molecular Engineering, Kyoto University.

[‡] Fukui Institute for Fundamental Chemistry.

[§] Institute for Integrated Cell-Material Sciences (iCeMS), Kyoto University.

- (1) The term *calixphyrin* was proposed by Sessler et. al to describe series of porphomethene, porphodimethene, porphotrimethene, and their analogues. Král, V.; Sessler, J. L.; Zimmerman, S. R.; Seidel, D.; Lynch, V.; Andrioletti, B. *Angew. Chem., Int. Ed.* **2000**, *39*, 1055.
- (2) (a) Senge, M. O.; Kalisch, W. W.; Bischoff, I. *Chem.—Eur. J.* **2000**, *6*, 2721. (b) Senge, M. O.; Runge, S.; Speck, M.; Ruhlandt-Senge, K. *Tetrahedron* **2000**, *56*, 8927. (c) Sessler, J. L.; Zimmerman, R. S.; Bucher, C.; Král, V.; Andrioletti, B. *Pure Appl. Chem.* **2001**, *73*, 1041. (d) Bischoff, I.; Feng, X.; Senge, M. O. *Tetrahedron* **2001**, *57*, 5573. (e) Senge, M. O. *Acc. Chem. Res.* **2005**, *38*, 733.
- (3) Bucher, C.; Zimmerman, R. S.; Lynch, V.; Král, V.; Sessler, J. L. *J. Am. Chem. Soc.* **2001**, *123*, 2099.

Scheme 1^a

^a (A) Calixphyrin, (B) heteroatom-containing hybrid calixphyrin, (C) P,S-containing hybrid calixphyrin, (D) palladium model complex of P,S-containing hybrid calixphyrin **1**, (E) palladium complex of P,S-containing hybrid porphyrin **2**, and (F) palladium complex of conventional porphyrin **3**.

containing hybrid calixphyrins (see Scheme 1B) are expected to provide both unprecedented properties and conformational flexibility. However, reports of heteroatom-containing hybrid calixphyrins have been limited so far.⁸

Also, the transition metal complex of heteroatom-containing hybrid calixphyrin and its reaction were not reported until the pioneering work reported recently by Matano et al.⁹ They succeeded in the synthesis of a series of P,S-containing hybrid calixphyrins that contain phosphole, thiophene, and pyrrole rings bridged by sp^2 - and sp^3 -hybridized meso carbons, as shown in Scheme 1C. These P,S-containing hybrid calixphyrins are expected to play a role of ligand for transition metal element, because phosphorus-, sulfur-, and nitrogen-containing macrocyclic mixed-donor ligands provide characteristic chelating sites that are difficult to construct with their acyclic analogues.^{10,11} Actually, they form palladium and rhodium complexes.^{9b} Interestingly, the palladium complex of P,S-containing hybrid calixphyrin catalyzes the Heck reaction which is one of typical Pd-catalyzed reactions.^{9a} Considering that even the palladium(0) species are not very reactive for oxidative addition,¹² the catalysis of this palladium complex for the Heck reaction is of considerable interest because the first step of this reaction is the oxidative addition.

Several theoretical studies of core-modified porphyrins have been reported. Delaere and Nguyen investigated the ground-

state electronic structure of unsubstituted monophospha- and diphosphaporphyrins with the DFT method and predicted the red-shifts of Q- and B-bands with the TD-DFT method.¹³ Matano et al. investigated the aromaticity of core-modified porphyrins¹⁴ and its transition metal complexes¹⁵ with the DFT method. However, no theoretical study of heteroatom-containing hybrid calixphyrins and their transition metal complexes has been reported yet.

In this theoretical study, we investigated the electronic structure of the palladium complex of a P,S-containing hybrid calixphyrin and the oxidative addition of phenyl bromide (PhBr) to its Pd center. Our purposes here are to clarify the electronic structure of this palladium complex, to elucidate how and why this palladium complex is reactive for the oxidative addition of PhBr, and to show the difference in the reactivity for the oxidative addition among palladium complexes of P,S-containing hybrid calixphyrin (Scheme 1D), P,S-containing hybrid porphyrin (Scheme 1E), and conventional porphyrin (Scheme 1F). We emphasize that this is the first theoretical study of a transition metal complex of heteroatom-containing hybrid calixphyrin and its reaction.

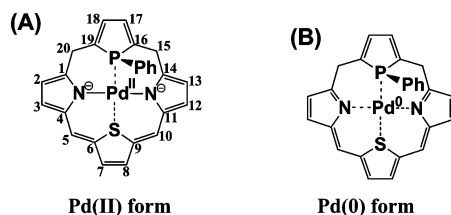
Computational Details

The DFT method with the B3LYP functional¹⁶ was used in this work, where two kinds of basis set system were used. In the smaller system (BS1) used for geometry optimization, core electrons of Pd (up to 3f) were replaced with effective core potentials (ECPs),¹⁷ and its valence electrons were represented with (311111/22111/411) basis set.¹⁷ For H, C, N, O, P, Cl, and S, 6-31G* basis sets were employed,¹⁸ where an anion function was added to each N and Cl because these atoms are anionic in the palladium complex of P,S-containing hybrid calixphyrin. For Br, the 6-311+G* basis set was employed, because the basis set effect is somewhat large in Br.²⁰ We ascertained that the combination of BS1 and B3PW91 presents reliable results in geometry optimization; see Tables S1–3 in Supporting Information.²¹ In the better basis set system (BS2) used for evaluation of energy changes, two f polarization functions were added to Pd with the same ECPs as those of BS1.^{17,22} For

- (8) Recently, the syntheses and structures of sulfur-containing phlorins were reported. Gupta, I.; Fröhlich, R.; Ravikanth, M. *Chem. Commun.* **2006**, 3726.
- (9) (a) Matano, Y.; Miyajima, T.; Nakabuchi, T.; Imahori, H.; Ochi, N.; Sakaki, S. *J. Am. Chem. Soc.* **2006**, *128*, 11760. (b) Matano, Y.; Miyajima, T.; Ochi, N.; Nakabuchi, T.; Shiro, M.; Nakao, Y.; Imahori, H.; Sakaki, S. *J. Am. Chem. Soc.* **2008**, *130*, 990. (c) Matano, Y.; Miyajima, T.; Ochi, N.; Nakao, Y.; Sakaki, S.; Imahori, H. *J. Org. Chem.* **2008**, *73*, 5139.
- (10) Recent reviews: (a) Caminade, A.-M.; Majoral, J. P. *Chem. Rev.* **1994**, *94*, 1183. (b) Dilworth, J. R.; Wheatley, N. *Coord. Chem. Rev.* **2000**, *199*, 89, and references therein.
- (11) (a) Fryzuk, M. D.; Kozak, C. M.; Bowdridge, M. R.; Jin, W.; Tung, D.; Patrick, B. O.; Retting, S. J. *Organometallics* **2001**, *20*, 3752. (b) Fryzuk, M. D.; Kozak, C. M.; Mehrhodavandi, P.; Morello, L.; Patrick, B. O.; Retting, S. J. *J. Am. Chem. Soc.* **2002**, *124*, 516. (c) Fryzuk, M. D.; Kozak, C. M.; Bowdridge, M. R.; Patrick, B. O.; Rettig, S. J. *J. Am. Chem. Soc.* **2002**, *124*, 8389. (d) Fryzuk, M. D.; Kozak, C. M.; Bowdridge, M. R.; Patrick, B. O. *Organometallics* **2002**, *21*, 5047.
- (12) (a) Louie, J.; Hartwig, F. J. *Angew. Chem., Int. Ed. Engl.* **1996**, *35*, 2359. (b) Louie, J.; Paul, F.; Hartwig, F. J. *Organometallics* **1996**, *15*, 2794.

- (13) Delaere, D.; Nguyen, M. T. *Chem. Phys. Lett.* **2003**, *376*, 329.
- (14) Matano, Y.; Nakabuchi, T.; Miyajima, T.; Imahori, H.; Nakano, H. *Org. Lett.* **2006**, *25*, 5713.
- (15) Matano, Y.; Nakabuchi, T.; Fujishige, S.; Nakano, Y.; Imahori, H. *J. Am. Chem. Soc.* **2008**, *130*, 16446.
- (16) (a) Becke, A. D. *J. Chem. Phys.* **1983**, *98*, 5648. (b) Becke, A. D. *Phys. Rev.* **1988**, *A38*, 3098. (c) Lee, C.; Yang, W.; Parr, R. G. *Phys. Rev.* **1988**, *B37*, 785.
- (17) Andrae, D.; Hauessermann, U.; Dolg, M.; Stoll, H.; Preuss, H. *Theor. Chim. Acta* **1990**, *77*, 123.
- (18) (a) Hehre, W. J.; Ditchfield, R.; Pople, J. A. *J. Chem. Phys.* **1972**, *56*, 2257. (b) Hariharan, P. C.; Pople, J. A. *Theor. Chim. Acta* **1973**, *28*, 213. (c) Hariharan, P. C.; Pople, J. A. *Mol. Phys.* **1974**, *27*, 209. (d) Francl, M. M.; Petro, W. J.; Hehre, W. J.; Binkley, J. S.; Gordon, M. S.; DeFrees, D. J.; Pople, J. A. *J. Chem. Phys.* **1982**, *77*, 3654.
- (19) Clark, T.; Chandrasekhar, J.; Spitznagel, G. W.; Schleyer, P. V. R. *J. Comput. Chem.* **1983**, *4*, 294.
- (20) Tuulmets, A.; Tammiku-Taul, J.; Burk, P. *J. Mol. Struct. (THEOCHEM)* **2004**, *674*, 233.
- (21) (a) We carried out geometry optimization with B3PW91, B3P86, and BLYP functionals, because they were reported to be useful for geometry optimization of the second-row transition-metal complexes.^{21b,c} (b) Waller, M. P.; Braun, H.; Hojdis, N.; Buhl, M. *J. Chem. Theory. Comput.* **2007**, *3*, 2234. (c) Schulz, N. E.; Zhao, Y.; Truhlar, D. G. *J. Phys. Chem. A* **2005**, *109*, 4388.
- (22) Martin, J. M. L.; Sundermann, A. *J. Chem. Phys.* **2001**, *114*, 3408.
- (23) (a) Krishnan, R.; Binkley, J. S.; Seeger, R.; Pople, J. A. *J. Chem. Phys.* **1980**, *72*, 650. (b) McLean, A. D.; Chandler, G. S. *J. Chem. Phys.* **1980**, *72*, 5639. (c) Blaudreau, J.-P.; McGrath, M. P.; Curtiss, L. A.; Radom, L. *J. Chem. Phys.* **1997**, *107*, 5016. (d) Curtiss, L. A.; McGrath, M. P.; Blandreau, J.-P.; Davis, N. E.; Binning, R. C.; Radom, L., Jr. *J. Chem. Phys.* **1995**, *103*, 6104.

Scheme 2



Br, the same basis set as that of BS1 was employed, and for H, C, N, O, P, Cl, and S, the 6-311G* basis sets²³ were employed, where an anion function was added to each N and Cl.^{19,23} The DFT/BS2-calculated enthalpy changes are given in this work, where vibrational frequencies were evaluated with the DFT/BS1 method.

In a model employed for calculation, four methyl groups on two sp^3 -carbon atoms and two phenyl groups on two meso carbon atoms of P,S-containing hybrid calixphyrin (Scheme 1C) were replaced with six H atoms, and the five-member ring fused with phosphole was replaced with two H atoms, because the P,S-containing hybrid calixphyrin is too large to optimize the transition state of reaction. The palladium complex of this model is named **1** hereafter; see Scheme 1D. Palladium complexes of the P,S-containing hybrid porphyrin and the conventional porphyrin are named **2** and **3**, respectively; see Schemes 1E and 1F. We selected **2** and **3** because they involve a P,S-containing well-conjugated macrocycle and a conventional porphyrin framework, respectively.

The Gaussian 03 program package²⁴ was used for all calculations. Population analysis was carried out with the method of Weinhold et al.²⁵ Molecular orbitals were drawn with the MOLEKEL program package.²⁶

Results and Discussion

Geometry and Electronic Structure of the Palladium Complex of P,S-Containing Hybrid Calixphyrin 1. As shown in Scheme 2, there are two kinds of valence tautomer in the palladium complex of P,S-containing hybrid calixphyrin **1**: one is a Pd(II) form (Scheme 2A), in which the calixphyrin moiety possesses -2 charges and the Pd center takes $+2$ oxidation state in a formal sense, and the other is a Pd(0) form (Scheme 2B), in which the calixphyrin moiety is neutral and the Pd center takes zero oxidation state. We investigated the electronic structure and the Pd oxidation state of **1**. The optimized geometry of **1** agrees well with the experimental one reported by Matano et al.,^{9a} as shown in Figure 1. Interestingly, the C^1-C^2 and C^3-C^4 distances are slightly longer than the C^2-C^3 distance in the pyrrole moiety, and the C^6-C^7 and C^8-C^9 distances are considerably longer than the C^7-C^8 distance in the thiophene moiety. Also, the C^4-C^5 distance is considerably longer than the C^5-C^6 distance. Optimized geometries of neutral P,S-containing hybrid calixphyrin **calix** and its dianion **calix**²⁻ are also shown in Figure 1. Significantly large differences are observed in C^1-C^2 , C^2-C^3 , C^4-C^5 , and C^5-C^6 bond distances between **calix** and **calix**²⁻; for instance, the C^1-C^2 distance is much longer in **calix** than in **calix**²⁻, while the C^2-C^3 distance is much shorter in **calix** than in **calix**²⁻. Also, the C^4-C^5 distance is much shorter than the C^5-C^6 distance in **calix** (Figure 1C) but much longer than the C^5-C^6 distance in **calix**²⁻ (Figure 1D). It is noted that the geometry of the calixphyrin moiety in

1 is similar to that of **calix**²⁻. These geometrical features of **1** suggest that the hybrid calixphyrin moiety possesses -2 charges and the Pd center takes $+2$ oxidation state in **1**; in other words, **1** takes the Pd(II) form.

To inspect the oxidation state of the Pd center, we compared natural atomic orbital (NAO) occupancy of the Pd center between **1** and typical Pd(II) model complex, *trans*-PdCl₂(C₄H₄S)(PPhC₄H₄) **1_M** (see Figure 1B), as shown in Table 1. The Pd oxidation state of **1_M** is $+2$ because of the presence of two Cl ligands. In **1_M**, the NAO occupancy of $d_{x^2-y^2}$ is 1.237 e and those of the other d_{xy} , d_{xz} , d_{yz} and d_{z^2} are 1.973 e, 1.996 e, 1.968 and 1.957 e, respectively, which are close to 2.0 e. In **1**, the NAO occupancy of $d_{x^2-y^2}$ is 1.233 e and those of the d_{xy} , d_{xz} , d_{yz} , and d_{z^2} are 1.960 e, 1.976 e, 1.963 e, and 1.935 e, respectively. These d-orbital populations of **1** are similar to those of **1_M**, suggesting that the Pd center takes $+2$ oxidation state in **1**.

To investigate the electronic structure of **1** in more detail, molecular orbitals (MOs) of **1** are represented by linear combination of MOs of fragments, Pd, and **calix**, as follows:

$$\psi_i(AB) = \sum_m C_{im}^A \varphi_m(A) + \sum_n C_{in}^B \varphi_n(B) \quad (1)$$

$$\rho_m(A) = \sum_i^{occ} [C_{im}^{A^2} + \sum_n C_{im}^A C_{in}^B S_{mn}] \quad (2)$$

where the $\psi_i(AB)$ is the *i*th MO of AB system such as **1**, $\varphi_m(A)$ is the *m*th MO of fragment A such as the Pd atom, and $\varphi_n(B)$ is the *n*th MO of fragment B such as **calix**. C_{im}^A and C_{in}^B are expansion coefficients of the $\varphi_m(A)$ and the $\varphi_n(B)$, respectively. The Mulliken-type population $\rho_m(A)$ represents how much electron population the $\varphi_m(A)$ possesses in the total system AB. This value is evaluated by eq 2, where the S_{mn} is the overlap integral between the $\varphi_m(A)$ and the $\varphi_n(B)$. As shown in Table 1, the Mulliken-type populations of the Pd d-orbital resemble well the NAO occupancies. It is noted that the Pd $d_{x^2-y^2}$ orbital population is much smaller than the other d-orbitals such as **1_M**, indicating that the Pd center takes $+2$ oxidation state (d^8 electron configuration) in a formal sense. Though the π^* (LUMO; see Figure 2) of neutral calixphyrin is unoccupied in free **calix**, its population is considerably large (1.464 e) in **1**, as shown in Table 1, indicating that the calixphyrin moiety in **1** takes a dianion form. However, the electron population of the LUMO is considerably smaller than the formal value of 2.0 for **calix**²⁻. This is because its electron population decreases by the charge transfer from the LUMO to the Pd $d_{x^2-y^2}$ orbital.²⁷ These results are consistent with the geometrical features discussed above. From all these results, it should be concluded that the calixphyrin moiety is dianion and the Pd center takes $+2$ oxidation state in **1**.

Geometry and Energy Changes in the Oxidative Addition of Phenyl Bromide (PhBr) to the Palladium Complex of P,S-Containing Hybrid Calixphyrin 1. Although the oxidation state of Pd is $+2$ in **1**, the Heck reaction whose first step is the oxidative addition of PhBr to the Pd center is catalyzed by **1**.^{9a} It is of considerable interest how and why the oxidative addition of PhBr to **1** occurs easily.

(24) Pople, J. A., et al. *Gaussian 03, revision C.02*, Gaussian, Inc.: Wallingford, CT, 2004.

(25) Reed, A. E.; Curtiss, L. A.; Weinhold, F. *Chem. Rev.* **1988**, *88*, 899.

(26) Flükiger, P.; Lüthi, H. P.; Portann, S.; Weber, J. MOLEKEL, v.4.3; Scientific Computing: Manno, Switzerland, 2002–2002. Portman, S.; Lüthi, H. P. *CHIMIA* **2000**, *54*, 766.

(27) The charge transfer from **calix**²⁻ to the Pd $d_{x^2-y^2}$ orbital considerably increases the electron population of the Pd $d_{x^2-y^2}$ orbital, as shown by the considerably large NAO occupancy of the $d_{x^2-y^2}$ orbital.

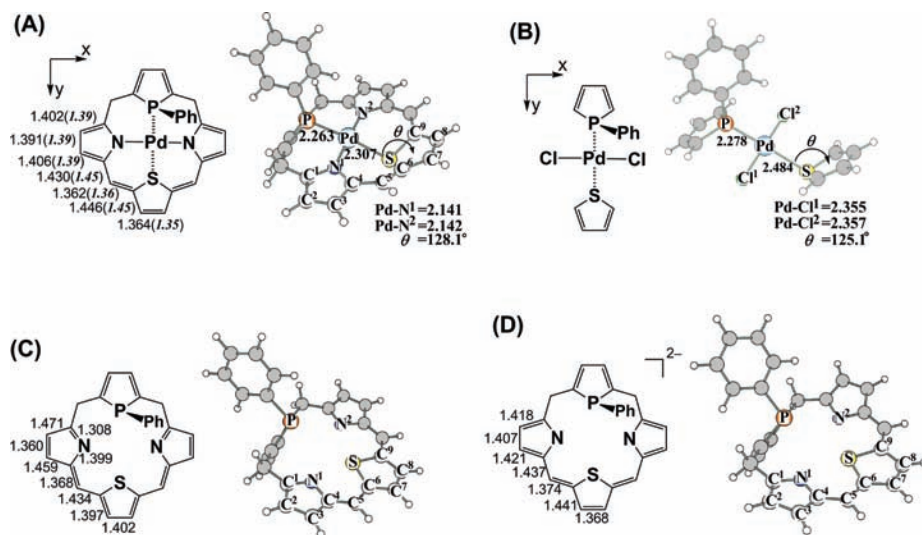


Figure 1. Optimized geometries of the (A) palladium complex of P,S-containing hybrid calixphyrin **1**, the (B) typical Pd(II) dichloro phosphole thiophene complex **1_M**, the (C) P,S-containing hybrid calixphyrin **calix**, and (D) its dianion **calix²⁻**. Bond lengths are in angstrom, and angles are in degrees. In parentheses are experimental values.^{9b} The geometries of **1**, **calix**, and **calix²⁻** are close to C₂ symmetry.

Table 1. Natural Atomic Orbital (NAO) Occupancies^a of **1_M** and **1** Evaluated with Weinhold's Method²⁵

		NAO occupancy		Mulliken population of 1 ^{a,b}
		1_M	1	
Pd	d _{xy}	1.973	1.960	1.934
	d _{xz}	1.996	1.976	1.926
	d _{yz}	1.968	1.963	1.949
	d _{z²}	1.957	1.935	1.915
	d _{x²-y²}	1.237	1.233	1.099
calixphyrin	π* ^b (LUMO)	—	—	1.464

^a The DFT(B3LYP)/BS2 was employed. ^b Mulliken population was estimated by eqs 2 and 3.

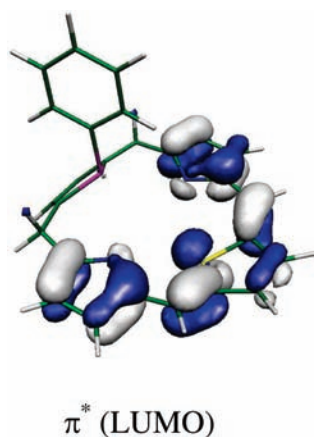
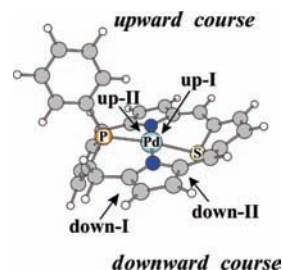


Figure 2. The π* (LUMO) orbital of P,S-containing hybrid calixphyrin fragment of **1**. The surface value is 0.04.

There are several possible approaching courses of PhBr to the Pd center, as shown in Scheme 3. In one course, PhBr approaches the Pd center on the same side of the phenyl group of the calixphyrin moiety, which is called the “upward course”. In the other course, PhBr approaches the Pd center on the opposite side of the phenyl group, which is called the “downward course”. In the upward course, PhBr approaches the Pd center in two ways: in one way (up-I), Ph and Br approach the positions trans to the S and P atoms, respectively. In the other (up-II), they approach the positions trans to the P and S atoms,

Scheme 3



respectively. The two similar approaching ways in the downward course are named down-I and down-II.

First, we will discuss the geometry changes in the up-I. PhBr approaches the Pd center of **1** to afford precursor complex **1PCa**, in which the Pd–Br distance is significantly long and the C–Br bond distance of PhBr is almost the same as that of free PhBr. These geometrical features indicate that the PhBr weakly interacts with the Pd center. Starting from **1PCa**, the PhBr further approaches the Pd center to afford intermediate **1INTa** through transition state **1TSa-I**, as shown in Figure 3A. Because the geometry of **1INTa** resembles well that of **1TSa-I**, **1TSa-I** is understood to be product-like, which is consistent with the fact that this process is considerably endothermic and the activation enthalpy is similar to the enthalpy change of reaction (see below). In **1TSa-I**, the Pd–Br distance decreases to 2.878 Å, which is much shorter than that of **1PCa**, and the Pd–N¹ distance moderately lengthens to 2.253 Å and the Pd–N² distance considerably lengthens to 2.970 Å. The distance (*h*) between the Pd center and the N¹–S–N² calixphyrin plane increases to 0.989 Å; in other words, the Pd center considerably moves upward above the N¹–S–N² plane. These geometrical features indicate that the interaction between the Pd center and the calixphyrin is becoming weak in **1TSa-I**. When going from **1PCa** to **1INTa**, the *h* distance considerably increases to 2.107 Å from –0.044 Å and the Pd–Br distance further shortens to 2.604 Å from 4.814 Å. The Pd–S, Pd–N¹, and Pd–N² distances considerably lengthen to 2.695 Å, 3.239 Å, and 3.244 Å from 2.308 Å, 2.141 Å, and 2.143 Å, respectively, while the Pd–P distance slightly shortens and the C–Br distance changes little in **1INTa**. These results indicate that pyrrole moieties do not

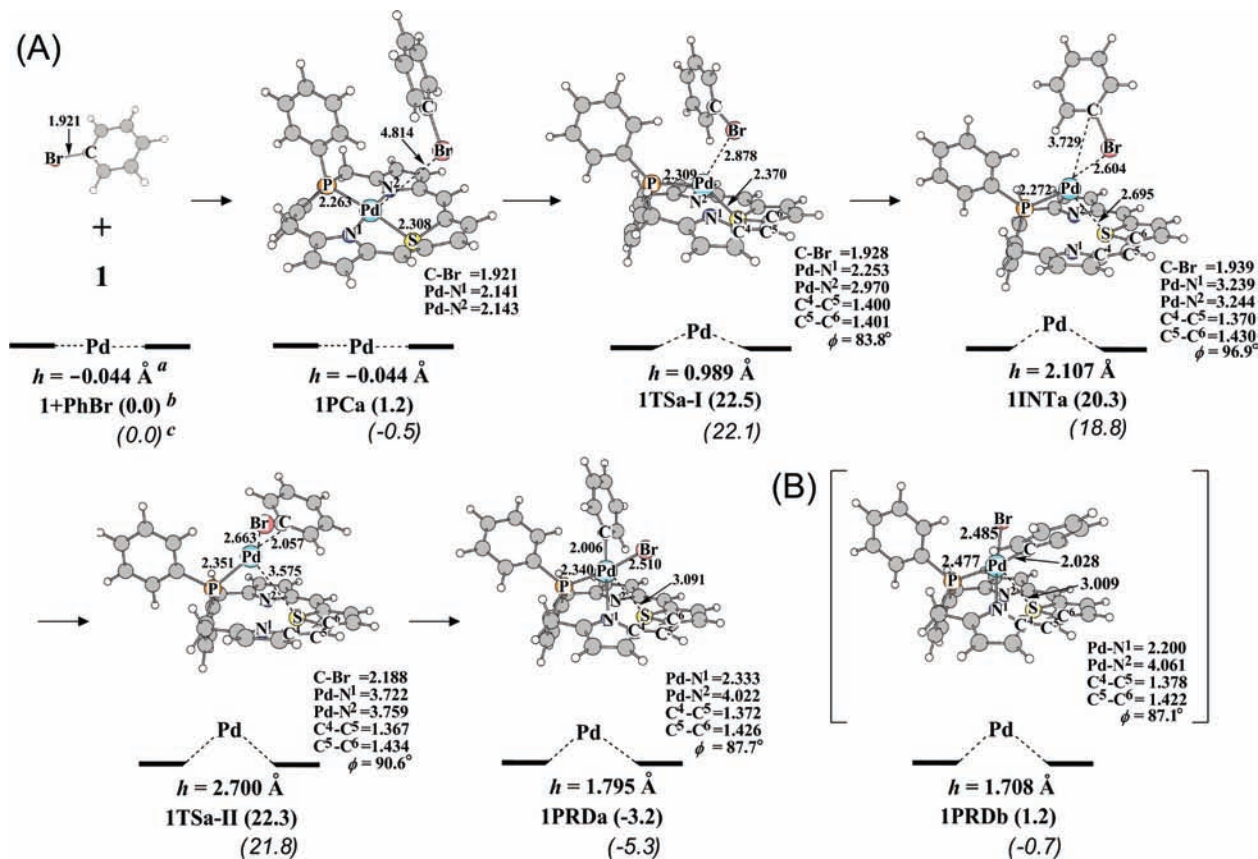


Figure 3. (A) Geometry changes in the oxidative addition of PhBr to the palladium complex of P,S-containing hybrid calixphyrin **1** through the up-I reaction course. (B) Geometry of **1PRDb** in the up-II reaction course. Bond lengths are in angstroms, and bond angles are in degrees. ^a The h indicates the distance between the Pd center and the N¹-S-N² plane. ^b The relative enthalpies (kcal/mol unit) to **1** + PhBr, where the DFT(B3LYP)/BS2 method was employed. ^c The energies with zero-point energy correction (kcal/mol unit) relative to **1** + PhBr, where the DFT(B3LYP)/BS2 method was employed.

coordinate to the Pd center and the hybrid calixphyrin plays a role of bidentate ligand in **1INTa**. Starting from **1INTa**, the C-Br σ -bond cleavage occurs through transition state **1TSa-II** to afford product **1PRDa**, as shown in Figure 3A. In **1TSa-II**, the C-Br distance of PhBr is elongated to 2.188 Å, which is moderately longer than that of **1INTa**. The Pd-C and Pd-Br distances decrease to 2.057 Å and 2.663 Å, respectively, which are considerably shorter than those of **1INTa** and similar to those of **1PRDa**. Also, the Pd-N¹, Pd-N², and Pd-S distances become considerably long but the Pd-P distance changes little. These geometrical features indicate that **1TSa-II** is understood to be a typical three-center transition state including a Pd monodentate phosphine ligand. In **1PRDa**, the Ph group and the Br atom take the positions trans to the N¹ atom and the phosphole moiety, respectively. The Pd-N¹ distance becomes considerably short (2.333 Å), which is the usual Pd-N coordinate bond distance. Thus, **1PRDa** is understood to be a four-coordinate complex.²⁸

We will omit detailed discussion of the geometry changes in the up-II but mention several important differences in geometry changes; see Supporting Information Figure S1 for geometry changes in the up-II. In the product **1PRDb** of this course, Ph and Br exist at the positions trans to the phosphole and the pyrrole, respectively, as shown in Figure 3B. It is noted that

the Pd-P bond distance is much longer in **1PRDb** than in **1PRDa** but the Pd-N¹ distance is much shorter in **1PRDb** than in **1PRDa**. These results indicate that the trans-influence effect of Ph is stronger than that of Br; note that the Ph group is at the position trans to the pyrrole in **1PRDa** but trans to the phosphole in **1PRDb**. Also, the Pd-Br distance is much longer in **1PRDa** than in **1PRDb**, indicating that the trans-influence effect of phosphole is stronger than that of pyrrole; note that the Br exists at the position trans to the phosphole in **1PRDa** but at the position trans to the pyrrole in **1PRDb**. Thus, **1PRDb** is less stable than **1PRDa**, as will be discussed below, because the Ph and the phosphole both possessing strong trans-influence effect exist at the positions trans to each other in **1PRDb** but at the positions cis to each other in **1PRDa**. The large difference is not, however, observed between **1TSa-II** and **1TSb-II**; see Figure 3 and Figure S1. This is because the Ph-Br bond cleavage has not been completed in **1TSa-II** and **1TSb-II**, and therefore the Ph moiety does not exhibit strong trans-influence effect yet. Also, **1TSa-I** is little different from **1TSb-I** in energy, because of the small trans-influence effect of PhBr; remember that the C-Br bond cleavage is not involved in **1TSa-I** and **1TSb-I**.

In the downward courses, we skip detailed discussion except for the difference in geometry changes of the up-I and up-II, because the down-I and down-II are less favorable than the up-I and up-II, respectively. One of the important differences between the upward reaction courses and the downward ones is that the Pd center moves downward below the N¹-S-N² plane unlike in the up-I and up-II courses; see Supporting Information Figures

(28) We examined another possible product in which Pd coordinates with the thiophene, and Ph and Br take the positions trans to S and N¹ atoms, respectively. However, this product is considerably less stable than **1PRDa** by 10.9 kcal/mol; see Figure S5 in Supporting Information.

Table 2. Activation Enthalpy (ΔH^{\ddagger})^a and Enthalpy Change of Reaction (ΔH^0)^b in the Oxidative Addition of Phenyl Bromide (PhBr) to the Palladium Complex of P,S-Containing Hybrid Calixphyrin **1** through up-I, up-II, down-I, and down-II

	up-I	up-II	down-I	down-II
ΔH^{\ddagger}	22.5	23.0	40.0	40.6
ΔH^0	-3.2	1.2	9.1	12.2

^a The difference between the highest transition state and the sum of reactant, because the precursor complex is less stable than the sum of reactant in enthalpy. ^b The difference between the product state and the sum of reactant. The DFT(B3LYP)/BS2 method was employed (in kcal/mol).

S2 and S3 for the geometry changes. Except for this difference, the oxidative addition of PhBr occurs similarly to that of the up-I and up-II courses.

Activation enthalpy (ΔH^{\ddagger}) and enthalpy change of reaction (ΔH^0) were calculated as the enthalpy difference between **ITSn-I** ($n = a, b, c, \text{ or } d$) and the sum of reactants and that between **1PRDn** and the sum of reactants, respectively, because **ITSn-I** is more unstable than **ITSn-II** and the **1PCn** is slightly less stable than the sum of reactants in enthalpy (see Figures 3, S1, S2, and S3). The negative ΔH^0 value represents that the reaction is exothermic. The ΔH^{\ddagger} value is moderate, 22.3 and 23.0 kcal/mol for the up-I and up-II, respectively, as shown in Table 2, though it is considerably large, 40.0 kcal/mol and 40.6 kcal/mol for the down-I and down-II, respectively. From these results, it should be concluded that the upward courses are much easier than the downward courses. The reason why the upward courses are easier than the downward ones is interpreted in terms of the position change of the Pd center; see Supporting Information pages S9–S11.

In summary, the oxidative addition of PhBr to **1** occurs through the up-I with moderate activation enthalpy. Although the activation enthalpy is little different between the up-I and up-II, the up-I is more favorable than the up-II from the thermodynamic viewpoint.

Changes in Electronic Structure Induced by the Oxidative Addition of PhBr to 1. It is of considerable interest to clarify the electronic process of the oxidative addition of PhBr to **1**. First, we investigated the electron population changes in this reaction, as shown in Figure 4A. Several characteristic features are summarized, as follows: (1) The Pd d-orbital population slightly decreases when going from **1** to **1PCa** and then considerably increases when going to **1INTa** from **1PCa**. Going from **1INTa** to **1PRDa**, the d-orbital population considerably decreases, and finally it becomes almost the same as that of **1**. (2) The electron population of the calixphyrin slightly increases when going from **1** to **1PCa** but considerably decreases when going to **1PRDa** from **1PCa**. (3) Although the electron populations of Ph and Br little change upon going to **1INTa** from **1PCa**, their populations considerably increase when going from **1INTa** to **1PRDa**. These population changes suggest that the Pd d-orbital receives electron population from the calixphyrin moiety when going to **1INTa** from **1**, and then charge transfer occurs from the Pd d-orbital to the PhBr when going from **1INTa** to **1PRDa**.

To present better understanding of population changes, we analyzed the molecular orbital $\psi_i(\text{ABC})$ of total system ABC with a linear combination of molecular orbitals of fragments A, B, and C, as shown in eq 3, where $\psi_i(\text{ABC})$ represents the i th MO of the total system **1**•••PhBr, $\varphi_m(\text{A})$ is the m th MO of the Pd atom, $\varphi_n(\text{B})$ is the n th MO of PhBr, and $\varphi_l(\text{C})$ is the l th MO of the calixphyrin. Orbital populations, $\rho_m(\text{A})$, $\rho_n(\text{B})$, and $\rho_l(\text{C})$, are evaluated with eqs 4–6. As shown in Figure 4B, the

electron population of the π orbital of calixphyrin does not change at all in this reaction. On the other hand, the electron population of the π^* orbital of the calixphyrin decreases to nearly zero when going to **1INTa** from **1PCa**, and simultaneously the Pd d-orbital population considerably increases. These results clearly indicate that the charge transfer considerably occurs from the π^* orbital of the calixphyrin moiety to the Pd d-orbital when going to **1INTa** from **1PCa**. As a result, both the calixphyrin moiety and the Pd atom become nearly

$$\psi_i(\text{ABC}) = \sum_m C_{im}^A \varphi_m(\text{A}) + \sum_n C_{in}^B \varphi_n(\text{B}) + \sum_l C_{il}^C \varphi_l(\text{C}) \quad (3)$$

$$\rho_m(\text{A}) = \sum_i^{occ} [C_{im}^A]^2 + \sum_n C_{im}^A C_{in}^B S_{mn}^{AB} + \sum_l C_{im}^A C_{il}^C S_{ml}^{AC} \quad (4)$$

$$\rho_n(\text{B}) = \sum_i^{occ} [\sum_m C_{in}^B C_{im}^A S_{mn}^{AB} + C_{in}^B] + \sum_l C_{in}^B C_{il}^C S_{nl}^{BC} \quad (5)$$

$$\rho_l(\text{C}) = \sum_i^{occ} [\sum_m C_{il}^C C_{im}^A S_{ml}^{AC} + \sum_n C_{in}^B C_{il}^C S_{nl}^{BC} + C_{il}^C] \quad (6)$$

neutral in **1INTa**. Going to **1PRDa** from **1INTa**, the Pd d-orbital population considerably decreases but the electron population of the Ph-Br σ^* orbital considerably increases, as shown in Figure 4B. In other words, the charge transfer occurs from the π^* orbital of the calixphyrin to the Pd d-orbital to afford the Pd(0) form when going to **1INTa** from **1PCa**. Then, the charge transfer occurs from the Pd d-orbital to the σ^* orbital of Ph-Br to induce the Ph-Br bond cleavage when going to **1PRDa** from **1INTa**. In **1PRDa**, the oxidation state of Pd becomes +2 again.

In summary, the oxidative addition to **1** occurs easily, because the Pd center changes to zero-oxidation state from +2 oxidation state when going to **1INTa** from **1** due to the charge transfer from the LUMO (π^*) orbital of the P,S-containing hybrid calixphyrin to the Pd d-orbital.

Oxidative Addition of PhBr to Palladium Complex of P,S-Containing Hybrid Porphyrin 2 and That of Conventional Porphyrin 3. We investigated the oxidative additions of PhBr to the similar palladium(II) complex of P,S-containing hybrid porphyrin **2** and that of conventional porphyrin **3**, to make comparison of **1** with **2** and **3**; see Scheme 1E and 1F for **2** and **3**, respectively. In the oxidative addition to **2**, PhBr approaches the Pd center to form precursor complex **2PC**; see Figure S6 in Supporting Information. Then, the PhBr further approaches the Pd center through transition state **2TS-I** to form intermediate **2INT**. In **2TS-I**, the Pd center considerably moves upward. The activation enthalpy is 43.3 kcal/mol, indicating that the position change of Pd is very difficult. Then, the C–Br σ -bond cleavage occurs through **2TS-II** to afford product **2PRD**. The geometry of **2TS-II** is similar to that of **1TSa-I**. Because **2INT** is much more unstable than **2PC**, the total activation enthalpy to complete the reaction is the energy difference between **2TS-II** and the sum of reactants. This activation enthalpy is 49.1 kcal/mol and the enthalpy change of reaction is 18.1 kcal/mol, indicating that the oxidative addition to **2** is difficult.

In the oxidative addition to **3**, intermediates such as **1INTa** are not formed; see Figure S7 for the geometry changes. In precursor complex **3PC**, PhBr is considerably distant from the

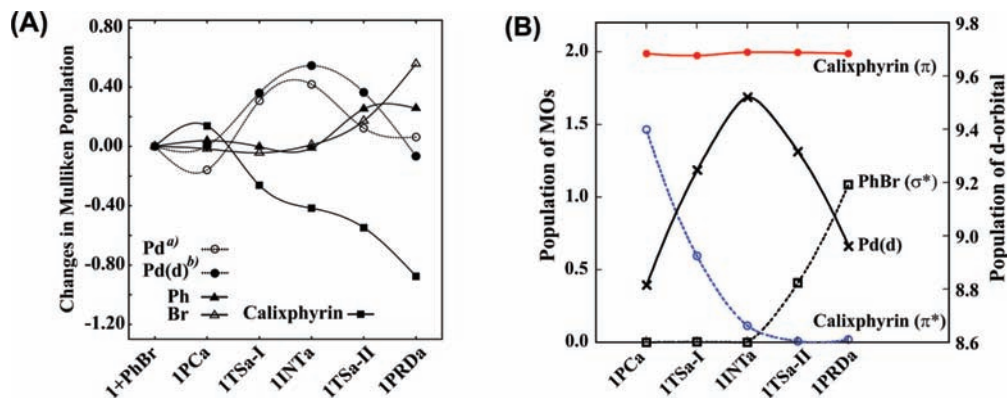


Figure 4. (A) Changes in Mulliken population and (B) population changes of MOs of fragments in the oxidative addition of PhBr to the palladium complex of P,S-containing hybrid calixphyrin **1**. The positive value represents the increase in electron population and vice versa. The DFT(B3LYP)/BS2 method was employed. ^aPopulation of Pd atom. ^bPopulation of d-orbital of Pd atom.

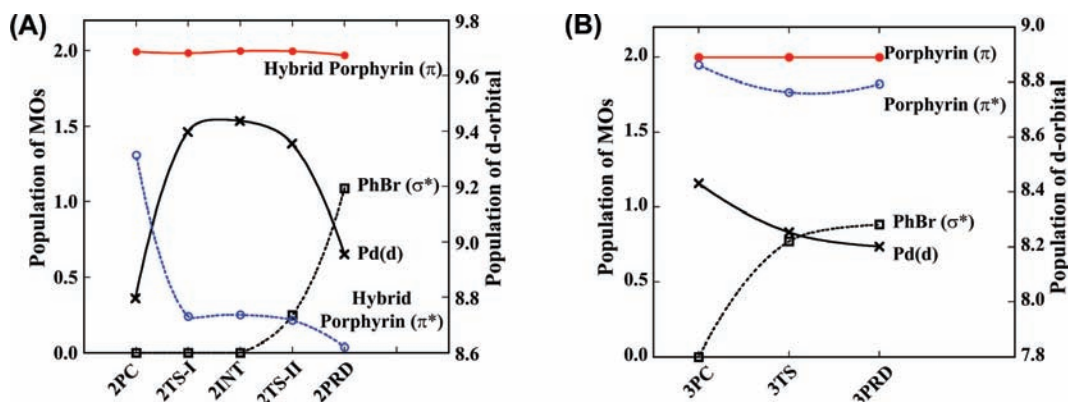


Figure 5. Population changes of important MOs of fragments in the oxidative addition of PhBr to (A) the palladium complexes of P,S-containing hybrid porphyrin **2** and (B) conventional porphyrin **3**. The DFT(B3LYP)/BS2 method was employed.

Pd center. Starting from **3PC**, the C–Br σ -bond cleavage occurs through transition state **3TS** to yield product **3PRD**. In **3TS**, the C–Br distance (2.831 Å) of PhBr is considerably elongated, and the Pd–C and Pd–Br distances are similar to those of **3PRD**. These features indicate that **3TS** is product-like. Consistent with these geometrical features, the activation enthalpy (74.4 kcal/mol) and the enthalpy change of reaction (74.6 kcal/mol) are very large. In **3PRD**, the porphyrin moiety is considerably distorted and the Pd center moderately moves upward. It is concluded that the oxidative addition of PhBr to **3** is very difficult, in contrast to **1**.

Reasons Why Palladium Complex of P,S-Containing Hybrid Calixphyrin Is Reactive for the Oxidative Addition, but Palladium Complexes of P,S-Containing Hybrid Porphyrin and Conventional Porphyrin Are Not. In the oxidative addition to **2**, the π^* orbital population of P,S-containing hybrid porphyrin considerably decreases and the Pd d-orbital population considerably increases when going to **2INT** from **2**, as shown in Figure 5A. Then, the σ^* orbital population of PhBr considerably increases with concomitant decrease of the Pd d-orbital population when going to **2PRD** from **2INT**. These population changes are essentially the same as those of the oxidative addition to **1**, though the oxidative addition of PhBr to **2** is difficult unlike that to **1**.

In the oxidative addition to **3**, electron populations of porphyrin π and π^* orbitals are always about 2.0 e, as shown in Figure 5B, which indicates that charge transfer does not occur from the porphyrin moiety to the Pd center during the reaction. The Pd d-orbital population considerably decreases and the σ^*

orbital population of PhBr considerably increases when going to **3PRD** from **3PC**. These results indicate that the oxidation state of Pd changes from +2 to +4 in the reaction.

It is worth investigating the reasons of the differences among **1**, **2**, and **3**. Although the π orbital energies are close to -5.5 eV in P,S-containing hybrid calixphyrin, P,S-containing hybrid porphyrin, and conventional porphyrin, the π^* orbital energy is considerably different among them, as shown in Figure 6, where the π and π^* orbital energies are calculated without the Pd atom. The π^* orbital is doubly occupied in the Pd complexes **1**, **2**, and **3** and the conversion from the Pd(II) form to the Pd(0) form needs the charge-transfer from the doubly occupied π^* orbitals to the Pd d orbital, as discussed above. Because the π^* orbital energy of conventional porphyrin is much lower than those of P,S-containing hybrid calixphyrin and P,S-containing hybrid porphyrin, the charge-transfer from the π^* orbital to the Pd d-orbital occurs with much more difficulty in **3** than in **1** and **2**. Hence, the conversion of the Pd(II) form to the Pd(0) form is difficult in **3**. As a result, the Pd(II) center must change to Pd(IV) center in the oxidative addition to **3**, which is very difficult.

It is noted that the π^* orbital energy of P,S-containing hybrid porphyrin is similar to that of the hybrid calixphyrin in the geometry of **PC** but that of a conventional porphyrin is much more stable. These results suggest that the phosphole and thiophene moieties play an important role in raising the π^* orbital energy. The π^* orbital energy of hybrid calixphyrin considerably rises but that of hybrid porphyrin moderately rises when going from the geometry in **PC** to that in **INT**, though

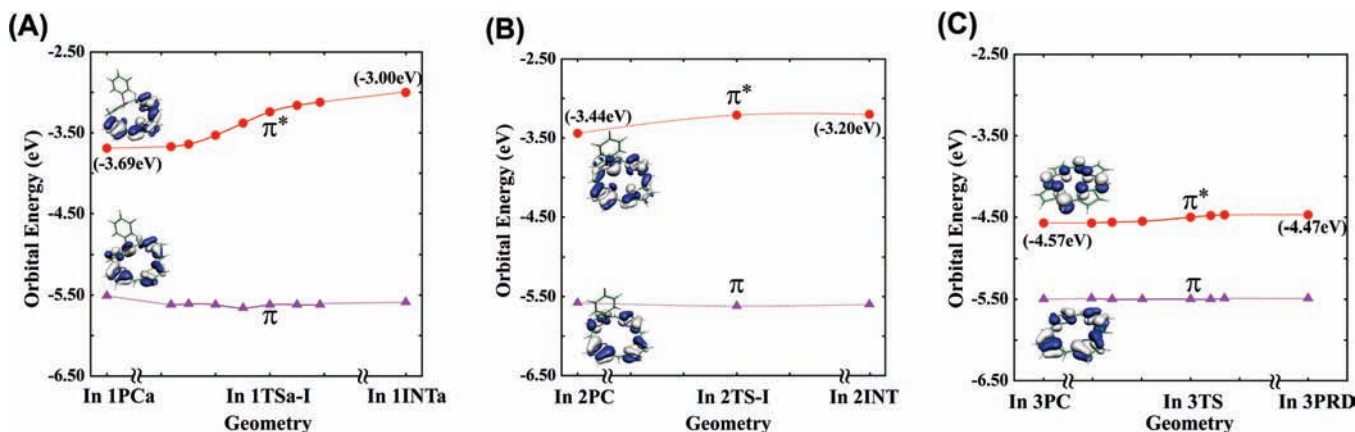


Figure 6. π and π^* orbital energies of (A) P,S-containing hybrid calixphyrin moiety, (B) P,S-containing hybrid porphyrin moiety, and (C) conventional porphyrin moiety, where the Pd atom is eliminated and the geometry is taken to be the same as the corresponding moiety of the palladium complex of P,S-containing hybrid calixphyrin **1**, the palladium complex of P,S-containing hybrid porphyrin **2**, and the conventional palladium porphyrin complex **3**. The DFT(B3LYP)/BS2 method was employed.

their π^* orbital energies are similar to each other in their equilibrium structures. These results indicate that the charge transfer from the π^* orbital of P,S-containing hybrid calixphyrin to the Pd d-orbital becomes easier than that from the P,S-containing hybrid porphyrin when going to **INT** from **PC**. This is because the π -conjugation of hybrid calixphyrin is interrupted by the presence of sp^3 -carbon atoms. On the other hand, the π^* orbital energy of hybrid porphyrin does not change easily, because the π -conjugation of hybrid porphyrin is strong due to the absence of the sp^3 -carbon atom.

From these results, it is concluded that the large reactivity of the palladium complex of P,S-containing hybrid calixphyrin **1** arises from the presence of the sp^3 -carbon atom and phosphole and thiophene moieties.

Comparison of Reactivity among 1, Palladium(0) Bisphosphine Complex Pd(PMe₃)₂ 4, and Palladium(II) Dichloro Bisphosphine Complex PdCl₂(PMe₃)₂ 5. We make the comparison of **1** with palladium(0) bisphosphine complex Pd(PMe₃)₂ **4** in the oxidative addition of PhBr. The geometry and energy changes of the oxidative addition to **4** are presented in Supporting Information Figure S9, because they were discussed previously.²⁹ The oxidative addition to **4** occurs with smaller activation enthalpy of 15.8 kcal/mol and larger enthalpy change of reaction (−18.0 kcal/mol) than those of the oxidative addition to **1**, indicating that **1** is less reactive for the oxidative addition than **4**. Also, we made the comparison of **1** with a typical palladium(II) complex, *trans*-PdCl₂(PMe₃)₂ **5**. The oxidative addition to **5** occurs with much larger activation enthalpy (51.2 kcal/mol) and much more positive enthalpy change of reaction (26.6 kcal/mol) than those of the oxidative addition to **1** (Supporting Information Figure S10). These results clearly indicate that **5** is much less reactive than **1**, similar to **2**, but more reactive than **3**; see above. It is likely that the larger reactivity of **5** than that of **3** arises from the more flexible geometry of **5** than that of **3**, indicating that the tight framework of the conventional porphyrin very much suppresses the oxidative addition. The activation enthalpy of the oxidative addition to **1** is only 2.0 kcal/mol relative to **1INTa**, which is similar to the activation enthalpy (0.5 kcal/mol) of the oxidative addition to a monodentate phosphine complex Pd(PMe₃) **6**; see Figure S11. This means that the large activation enthalpy for **1**

arises from the tautomerization from the Pd(II) form to the Pd(0) form, and the neutral form of the P,S-containing hybrid calixphyrin plays a role of ligand similar to monodentate phosphine.

Conclusions

There are two valence tautomers, Pd(II) form and Pd(0) form, in the palladium complex of P,S-containing hybrid calixphyrin **1**. The d-orbital populations indicate that **1** takes the Pd(II) form. Although the Pd(II) complex is unfavorable for the oxidative addition, the oxidative addition of PhBr to **1** occurs with moderate activation enthalpy, as follows: The valence tautomerization from the Pd(II) form to the Pd(0) form occurs concomitantly with the approach of PhBr to the Pd center and the position movement of the Pd center to afford intermediate **1INTa**. The activation enthalpy (20.3 kcal/mol) is moderate. Starting from the Pd(0) form, the C–Br σ -bond activation of PhBr easily occurs with small activation enthalpy of 2.0 kcal/mol, relative to **1INTa**.

Also, the oxidative addition to palladium complex of P,S-containing hybrid porphyrin **2** and that of conventional porphyrin **3** were investigated. The activation enthalpies are 49.1 and 74.4 kcal/mol in the reactions of **2** and **3**, respectively, which are much larger than that of **1**. In **1**, the tautomerization from the Pd(II) form to the Pd(0) form occurs with moderate activation enthalpy; see above. In other words, the oxidation state of Pd changes to zero from +2 prior to the oxidative addition. In **3**, the π^* orbital population decreases little, indicating that the Pd oxidation state cannot change to zero. In **2**, the charge transfer occurs from the π^* orbital to the Pd center by the tautomerization, while the activation enthalpy for this process is very large. These differences among **1**, **2**, and **3** are interpreted in terms of the π^* orbital energy and its dependency on the geometry change. It should be concluded that the higher reactivity of **1** for the oxidative addition arises from the presence of phosphole and thiophene moieties and sp^3 -carbon atoms in P,S-containing hybrid calixphyrin. Though **1** is more reactive than **2** and **3**, **1** is less reactive than palladium(0) bisphosphine complex Pd(PMe₃)₂ **4**. This is because the tautomerization from the Pd(II) form to the Pd(0) form needs large activation enthalpy.

Acknowledgment. This work was financially supported by Grant-in-Aids on Priority Areas for “Molecular Theory for Real Systems” (No.461) and NAREGI project from the Ministry of

(29) Fazaeli, R.; Ariafard, A.; Jamshidi, S.; Tabatabaie, E. S.; Pishro, K. A. *J. Organomet. Chem.* **2007**, *692*, 398.

Education, Science, Sports, and Culture. One of the authors (N. Ochi) thanks the Grant-in Aid for JSPS Fellows. Some of theoretical calculations were performed with SGI Altix4700 workstations of Institute for Molecular Science (Okazaki, Japan), and some of them were carried out with PC cluster computers of our laboratory.

Supporting Information Available: The full representation of ref 24. Optimized geometries of **1** with various basis sets (Tables S1 and S2). Optimized geometries of **1** with several functionals (Table S3). Geometry changes in up-II, down-I, and down-II (Figures S1–3). Potential energy surface against the dihedral angle ϕ between the phosphole moiety and calixphyrin plane in P,S-containing hybrid calixphyrin **1** (Figure S4). Geometry of another product **1PRD_s**, in which the Pd coordi-

nates to S and N¹ (Figure S5). Geometry changes in the oxidative addition of PhBr to the palladium complex of P,S-containing hybrid porphyrin **2** and that of conventional porphyrin **3** (Figures S6 and S7). Mulliken population changes in the oxidative addition of PhBr to **2** and **3** (Figure S8). Geometry changes in oxidative addition of PhBr to palladium(0) bisphosphine complex Pd(PMe₃)₂ **4** (Figure S9), palladium(II) dichloro bisphosphine complex PdCl₂(PMe₃)₂ **5** (Figure S10), and monodentate phosphine complex Pd(PMe₃) **6** (Figure S11). Calculated total energies (in Hartree units; Tables S4 and S5). Cartesian coordinates of all species (Table S6). This material is available free of charge via the Internet at <http://pubs.acs.org>.

JA901166A